PHOTONICS Research

Highly stable femtosecond pulse generation from a MXene $Ti_3C_2T_x$ (T = F, O, or OH) mode-locked fiber laser

Jie Li,[1,†] Zilong Zhang,[1,†] Lin Du,[1] Lili Miao,[1] Jun Yi,[1] Bin Huang,[1] Yanhong Zou,[1,2] Chujun Zhao,[1,3] and Shuangchun Wen[1]

[1]Key Laboratory for Micro/Nano Optoelectronic Devices of Ministry of Education & Hunan Provincial Key Laboratory of Low-Dimensional Structural Physics and Devices, School of Physics and Electronics, Hunan University, Changsha 410082, China
[2]e-mail: yanhongzou@hnu.edu.cn
[3]e-mail: cjzhao@hnu.edu.cn

Received 31 October 2018; revised 18 December 2018; accepted 23 December 2018; posted 2 January 2019 (Doc. ID 349316); published 7 February 2019

Ultrafast fiber lasers are in great demand for various applications, such as optical communication, spectroscopy, biomedical diagnosis, and industrial fabrication. Here, we report the highly stable femtosecond pulse generation from a MXene mode-locked fiber laser. We have prepared the high-quality $Ti_3C_2T_x$ nanosheets via the etching method, and characterized their ultrafast dynamics and broadband nonlinear optical responses. The obvious intensity- and wavelength-dependent nonlinear responses have been observed and investigated. In addition, a highly stable femtosecond fiber laser with signal-to-noise ratio up to 70.7 dB and central wavelength of 1567.3 nm has been delivered. The study may provide some valuable design guidelines for the development of ultrafast, broadband nonlinear optical modulators, and open new avenues toward advanced photonic devices based on MXenes.

https://doi.org/10.1364/PRJ.7.000260

1. INTRODUCTION

Stable ultrafast fiber lasers have become indispensable tools for a variety of applications, such as optical communication, spectroscopy, biomedical diagnosis, and industrial fabrication, for their excellent beam quality, efficient heat dissipation, compact configuration, and high-quality pulse generation [1–4]. To constitute a compact fiber laser, the saturable absorber (SA) plays a very important role in modulating laser systems to deliver an ultrafast laser. Inspired by the requirement of a stable, cost-effective ultrafast fiber laser, researchers from different communities try their best to develop novel SAs [5–7]. With the evolution of low-dimensional optical materials, graphene and other two-dimensional (2D) materials have become a hot research topic in recent years for their unique performance in the field of broadband optoelectronic devices resulting from their special electronic structure and excellent physical and chemical properties [8–14]. However, the lack of a well-controlled, stable preparation method remains a hurdle to applications of 2D materials and their optical properties; in particular, nonlinear optics still requires deeper understanding.

Recently, MXenes, a new series of 2D materials composed of early transition metal carbides and/or carbonitrides, was first introduced by Gogotsi's group in 2011 [15]. As a new family of 2D materials, MXenes have drawn extensive attention in many areas, such as energy storage, electromagnetic interference shielding, composite reinforcement, water purification, chemical catalysts, biosensors, photothermal therapy, and light-to-heat conversion for energy harvesting [16–19]. Delamination of MXenes produces single-layer nanosheets with thicknesses of about a nanometer and lateral sizes on the order of micrometers. Their general formula is $M_{n+1}X_nT_x$ ($n = 1$–3) [20], where M represents an early transition metal (such as Sc, Ti, Zr, Hf, V, Nb, Ta, Cr, or Mo), X is carbon and/or nitrogen, and T_x stands for the surface terminations (e.g., hydroxyl, oxygen, or fluorine). Compared with the typical 2D materials such as graphene and molybdenum sulfide, MXenes have the advantages of good hydrophilicity, metallic conductivity, and adjustable chemical composition [21,22]. When it comes to the optical regime, some theoretical and experimental works have been reported [23–25]. However, the optical nonlinearities and related applications of MXenes have been paid less attention.

Recently, Jhon *et al.* investigated the potential of MXene compounds for producing *Q*-switched and/or mode-locked laser pulses through a combined experimental and computational approach in which Ti_3CNT_x was used as a MXene-based SA [26]. Jiang *et al.* measured the third-order susceptibilities of

$Ti_3C_2T_x$ film by a Z-scan technique in the broadband range, and achieved mode-locked fiber lasers at 1066 nm and 1555 nm [27]. Tuo *et al.* found that 2D transition metal carbides α–Mo_2C crystals have excellent saturable absorption properties in terms of largely tunable modulation depth and very low saturation intensity [28]. Dong *et al.* experimentally found that $Ti_3C_2T_x$ has superior tunable saturable absorption properties, and MXenes are more resilient than other 2D materials with high damage thresholds [29].

In this work, we have synthesized $Ti_3C_2T_x$ (T = F, O, or OH) through an etching method. In addition, we have studied the ultrafast dynamics of the materials by transient absorption techniques, and investigated the nonlinear saturable absorption behavior of $Ti_3C_2T_x$ film by using the open aperture Z-scan technique from ultraviolet 400 nm to an optical communication window around 1550 nm. In addition, the stable ultrafast fiber laser has been delivered successfully by inserting the $Ti_3C_2T_x$ SA into an erbium-doped fiber laser cavity, with pulse duration down to 946 fs and signal-to-noise ratio (SNR) up to 70.7 dB at the central wavelength of 1567.3 nm.

2. PREPARATION AND CHARACTERIZATIONS OF $Ti_3C_2T_x$

MXene $Ti_3C_2T_x$ was prepared on the basis of the method reported by Naguib *et al.* [15]. In a typical process, Ti_3AlC_2 powders (≥98% purity; Beijing Lianlixin Technology Co., Ltd., China) were immersed in aqueous hydrogen fluoride (HF) solution (40%) for 48 h at room temperature. After washing with deionized water several times, the resulting deposition was dried in vacuum at 60°C for 48 h. As shown in Fig. 1(a), the X-ray diffraction (XRD) pattern validated the successful fabrication of a pure Ti_3AlC_2 phase, which is in accordance with the standard spectrum (JCPDS 52-0875) [30].

After HF etching, the strongest XRD peak, e.g., (104), in the out-of-plane direction was significantly weakened, and a broader peak of (002) corresponding to in-plane diffraction appeared at a 2θ angle of 8.9° in $Ti_3C_2T_x$, indicating substantial expansion of the interlayer spacing from 9.3 Å (1 Å = 0.1 nm) for Ti_3AlC_2 to 9.9 Å for $Ti_3C_2T_x$ [15]. The linear absorption of the $Ti_3C_2T_x$ sample is characterized by the spectrometer (Shimadzu ISR-603) in Fig. 1(b), which shows that $Ti_3C_2T_x$ has a big and relatively flat absorption from ultraviolet to mid-infrared. Scanning electron microscopy (SEM) shows that the material has a layered structure, and the exfoliated layer is relatively large, as shown in Figs. 1(c) and 1(d). In Fig. 1(e), the interlayer distance is determined as 9.85 Å, matching well with the previous theoretical value (9.93 Å) [31]. As shown in Fig. 1(f), the transmission electron microscope (TEM) analysis of the exfoliated nanosheets shows that they are quite thin and transparent to electrons.

3. ULTRAFAST DYNAMICS AND BROADBAND SATURABLE ABSORPTION OF $Ti_3C_2T_x$

We have characterized the ultrafast dynamics of the $Ti_3C_2T_x$ via the femtosecond transient absorption spectrum, which is very important for potential ultrafast applications [32,33]. During the measurement, the 400 nm laser acts as the pump

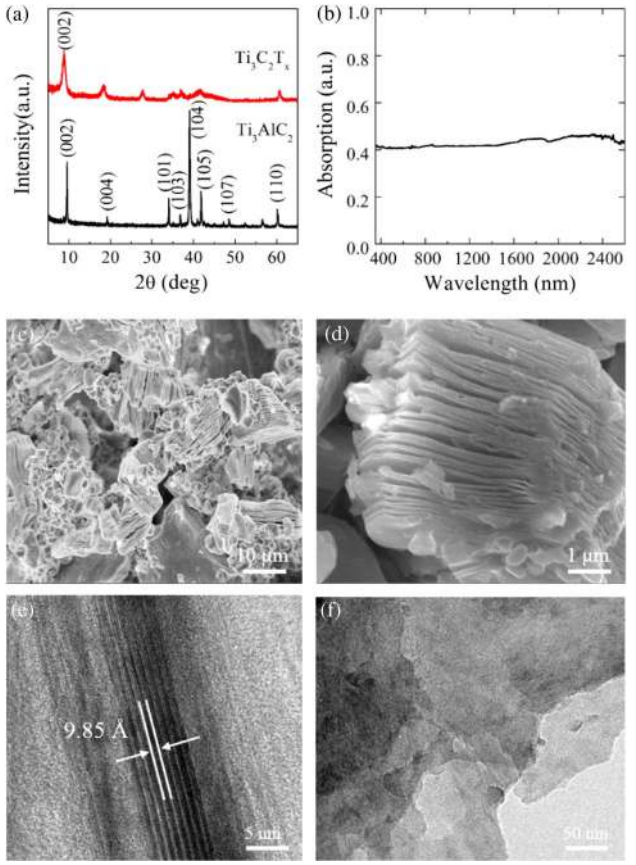

Fig. 1. (a) XRD patterns of the $Ti_3C_2T_x$ and Ti_3AlC_2. (b) Linear absorption spectrum of $Ti_3C_2T_x$. (c), (d) SEM images of delaminated $Ti_3C_2T_x$ after HF etching under different magnifications. (e) Interlayer distance is measured to be 9.85 Å. (f) TEM image of the $Ti_3C_2T_x$ flakes.

light, and the super continuum white light acts as the probe light. With the help of the time delay line, the transient absorption curves can be obtained, as shown in Fig. 2. The change in the absorption intensity obtained by the experiment is represented by the change in optical density $\Delta OD = \lg \frac{I_{nopump}}{I_{pump}}$, where I_{nopump} is the intensity of light detected when there is no pump light, and I_{pump} is the intensity of light detected when the pump light is on. In Fig. 2(a), the signal appears negative for a long time, and the valley around 650 nm shows no significant shift with time delay, exhibiting mainly saturable absorption. We have extracted the photodynamic curve of the sample at 650 nm from the transient absorption curve, as shown in Fig. 2(b). By fitting the experimental results [34], two relaxation times can be obtained. After the pump laser pulse is applied, the curve drops and recovers rapidly, with a lifetime of 0.81 ps, and then stabilizes slowly after 28.8 ps. The ultrafast recovery time makes $Ti_3C_2T_x$ a promising nonlinear optical material for ultrafast applications, particularly as an effective SA in a mode-locked fiber laser.

To investigate the broadband nonlinear optical properties, a $Ti_3C_2T_x$-methanol solution was spin-coated onto 1 mm thick quartz glass. Then we experimentally investigated the saturable absorption property of the $Ti_3C_2T_x$ using the open aperture

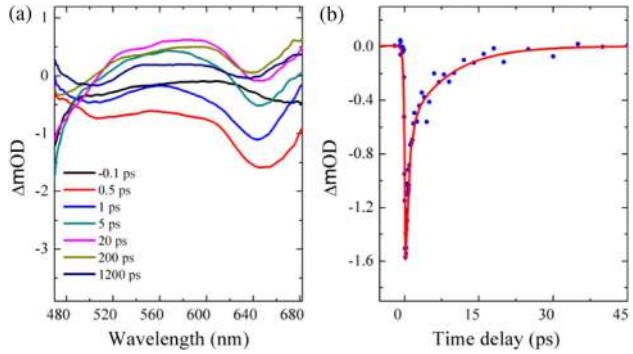

Fig. 2. Ultrafast dynamic process of the $Ti_3C_2T_x$ sample. (a) Transient absorption curve of the sample and (b) photodynamic curve of the sample.

Z-scan technique. The experimental setup is shown in Fig. 3. The ultrafast pulses have been delivered from two lasers (laser 1: center wavelength: 800 nm, pulse duration: 100 fs, 3 dB spectral width: 15 nm, and repetition rate: 1 kHz; laser II: center wavelength: 1560 nm, pulse duration: 100 fs, 3 dB spectral width: 10 nm, and repetition rate: 80 MHz). By frequency doubling, the experimental irradiation source adopted can cover the ultraviolet to near-infrared band. During the experiment, the 5:5 beam splitter can divide the laser beam into two paths. One beam is collected by detector 1 as a reference beam, and the other beam passes through the $Ti_3C_2T_x$ sample with a focal length of 500 mm and is collected by detector 2. According to the CS_2 measurement, the incident beam waist is fitted to be about 55 μm. During the experiment, the sample surface is perpendicular to the incident laser beam and moves back and forth around the beam focus.

The open aperture Z-scan measurements with the $Ti_3C_2T_x$ sample are shown in Fig. 4. When the $Ti_3C_2T_x$ sample approaches the beam focus, the normalized transmittance gradually increases. This shows that as the incident pump intensity increases, the light absorption of the sample becomes smaller and gradually becomes saturated. By using optical attenuators, the average power could be deliberately controlled. As shown in Figs. 4(a), 4(c), and 4(e), the peaks of the open-aperture Z-scan curves increase with the increase of the input peak intensity.

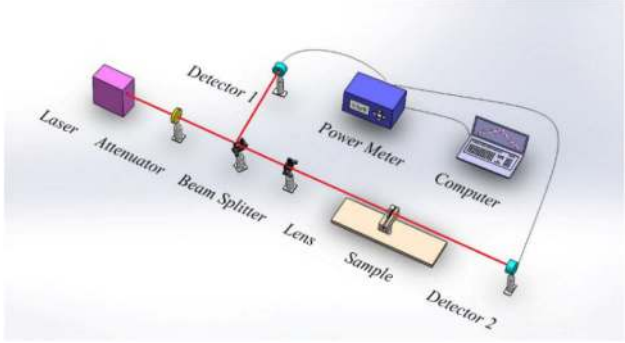

Fig. 3. Experiment setup of open aperture Z-scan measurements with the $Ti_3C_2T_x$ sample.

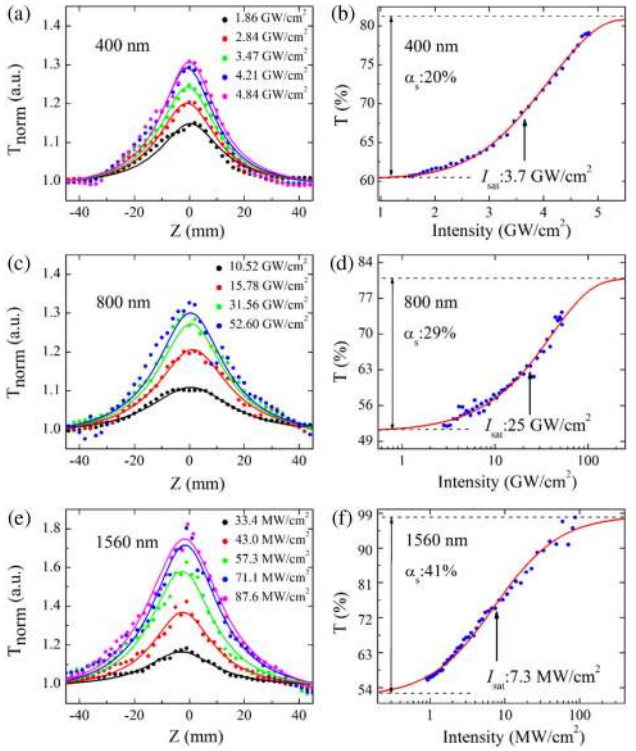

Fig. 4. Broadband nonlinear saturable absorption properties of $Ti_3C_2T_x$. Open aperture Z-scan measurements of $Ti_3C_2T_x$ sample under different intensities at (a) 400 nm, (c) 800 nm, and (e) 1560 nm, respectively; relationship between transmittance and input intensity at (b) 400 nm, (d) 800 nm, and (f) 1560 nm, respectively.

In Figs. 4(b), 4(d), and 4(f), we fit the experimental data with a typical nonlinear transmission function of an SA depending on the incident light intensity. The transmittance T has a relationship with input optical intensity I as [35]

$$T = 1 - \left(\frac{\alpha_s}{1 + I/I_{\text{sat}}} + \alpha_{\text{ns}}\right), \tag{1}$$

where α_s is the modulation depth, α_{ns} is the non-saturable components, and I_{sat} is the saturable intensity. The experimental data match quite well with Eq. (1). By fitting the experimental results, it was found that the modulation depth and saturable intensity are about 20% and 3.7 GW/cm^2 at 400 nm, 29% and 25 GW/cm^2 at 800 nm, and 41% and 7.3 MW/cm^2 at 1560 nm, respectively. The layered $Ti_3C_2T_x$ nanosheets exhibited properties ranging from metals to semiconductors due to the different surface groups [15]. The experimental results show that in the optical communication band where the photon energy is relatively small, the nonlinear absorption exhibits a large modulation depth [36]. By taking advantage of the saturable absorption property, $Ti_3C_2T_x$ could be developed as broadband passive nonlinear optical modulators [1].

4. ULTRAFAST LASERS MODULATED BY $Ti_3C_2T_x$

With a fiber laser configuration with a cavity length of 24.8 m, as shown in Fig. 5, self-started mode-locking operation with a

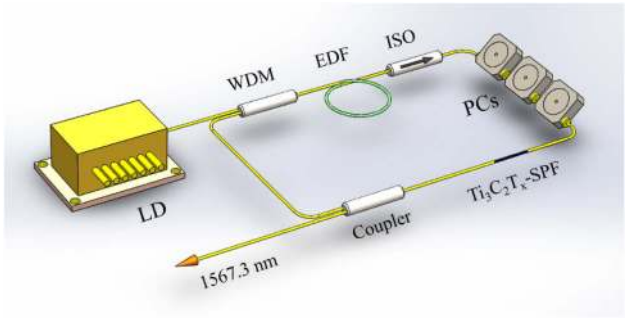

Fig. 5. Experimental setup of the $Ti_3C_2T_x$-based mode-locked erbium-doped fiber laser.

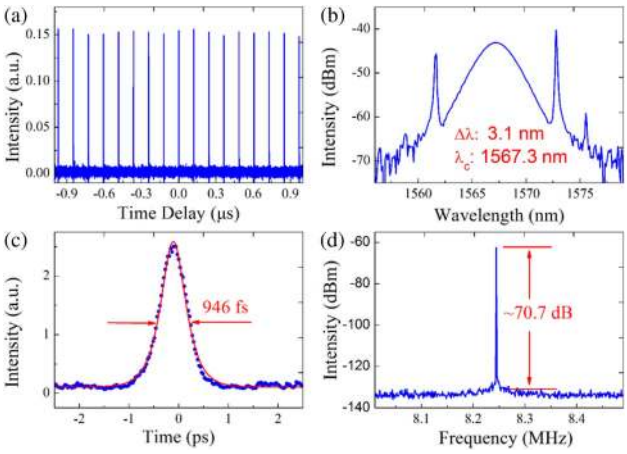

Fig. 6. Results of mode locking. (a) Pulse train, (b) spectrum of mode locking, (c) autocorrelation trace, and (d) RF spectrum.

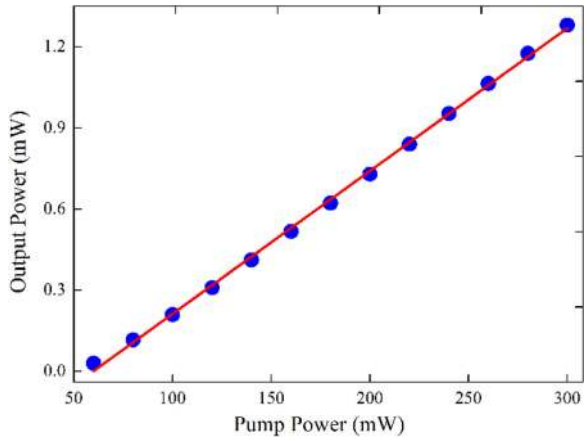

Fig. 7. Output power versus pump power.

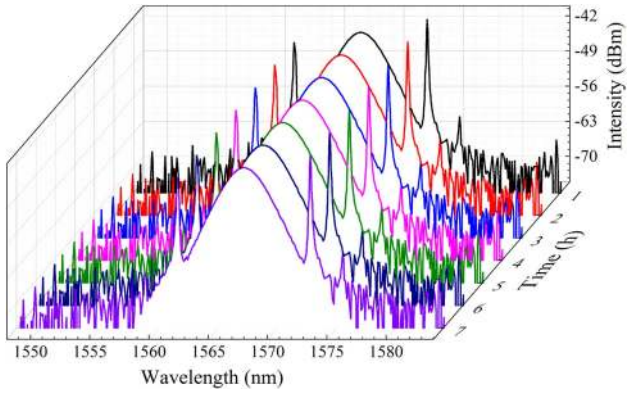

Fig. 8. Output spectra collection across 7 h.

threshold pump of 55 mW has been obtained. In the laser cavity, we used a piece of 0.9 m erbium-doped fiber with a group velocity dispersion (GVD) parameter of 15.8 ps/(nm·km) and 23.9 m standard single-mode fiber with a GVD parameter of 18 ps/(nm·km) at 1550 nm. The pump from a 975 nm laser diode (LD) source was coupled into the cavity through a 980/1550 wavelength-division multiplexer (WDM), and a 10% fiber coupler was employed to deliver the laser emission. We incorporated the $Ti_3C_2T_x$-based side-polished fiber (SPF) that has a modulation depth of 41% and a saturable intensity of 7.3 MW/cm^2 in the fiber cavity. Figure 6 summarizes the characteristics of the mode-locking operation of the fiber laser at a pump power of 60 mW. Figure 6(a) shows the single-pulse train recorded over 2 μs. The pulses have a repetition rate of 8.24 MHz, which matches well with the cavity length, indicating that the laser operates in the mode-locking state. The corresponding optical spectrum, as shown in Fig. 6(b), has obvious Kelly spectral sidebands, indicating that the fiber laser is operating in the soliton regime. It has a central wavelength of 1567.3 nm and a 3 dB bandwidth of 3.1 nm. Correspondingly, as shown in Fig. 6(c), the measured autocorrelation (AC) trace can be well fitted by the hyperbolic secant function with a full width at half maximum (FWHM) of 1.46 ps, indicating that the real pulse width is about 946 fs. The time-bandwidth product is 0.358, showing that the obtained soliton pulse is almost transform limited. Figure 6(d) is the corresponding radio frequency (RF) spectrum with a resolution bandwidth (RBW) of 10 Hz. The SNR is as high as 70.7 dB, which shows stable mode-locking operation compared to the previously reported 1.5 μm pulsed laser [26–28]. We measured the output power of the mode-locked fiber laser, as shown in Fig. 7. It can be seen that 10% of the output power of the mode-locked fiber laser linearly increases as the pump power increases. The high SNR manifests that the MXene SA can be an ideal candidate for ultrashort pulse laser generation.

To investigate the long-term stability of the single-soliton operation, we recorded the output spectra every hour over 7 h under a fixed experimental condition, such as pump power of 60 mW, as shown in Fig. 8. Neither the central wavelength drifted nor a new wavelength component was generated during the measurement, showing excellent repeatability and long-term stability.

5. CONCLUSION

In summary, we have prepared the few-layer $Ti_3C_2T_x$ by a simple and quick etching method. In addition, we experimentally studied the transient absorption behavior and systematically

investigated the broadband saturable absorption property of $Ti_3C_2T_x$ from 400 nm to 1560 nm using the Z-scan technique. We further used few-layer $Ti_3C_2T_x$ as an SA to mode lock an erbium-doped fiber laser, and a stable femtosecond laser pulse has been successfully obtained with a SNR up to 70.7 dB. Our experimental results demonstrated that $Ti_3C_2T_x$ could be a potential candidate for a broadband stable nonlinear optical modulator and can open new avenues toward advanced photonic devices based on MXenes.

Funding. National Natural Science Foundation of China (NSFC) (11574079, 61475102, 61775056); Natural Science Foundation of Hunan Province (2017JJ1013); Ministry of Education of the People's Republic of China (MOE) (6141A02033404).

†These authors contributed equally to this work.

REFERENCES

1. U. Keller, "Recent developments in compact ultrafast lasers," Nature **424**, 831–838 (2003).
2. W. Yang, P. G. Kazansky, and Y. P. Svirko, "Non-reciprocal ultrafast laser writing," Nat. Photonics **2**, 99–104 (2008).
3. M. Malinauskas, A. Zukauskas, S. Hasegawa, Y. Hayasaki, V. Mizeikis, R. Buividas, and S. Juodkazis, "Ultrafast laser processing of materials: from science to industry," Light Sci. Appl. **5**, e16133 (2016).
4. R. Osellame, H. J. W. M. Hoekstra, G. Cerullo, and M. Pollnau, "Femtosecond laser microstructuring: an enabling tool for optofluidic lab-on-chips," Laser Photon. Rev. **5**, 442–463 (2011).
5. H. Zhang, Q. Bao, and Z. Sun, "Introduction to two-dimensional layered materials for ultrafast lasers," Photon. Res. **6**, TDL1–TDL2 (2018).
6. A. Martinez and Z. Sun, "Nanotube and graphene saturable absorbers for fiber lasers," Nat. Photonics **7**, 842–845 (2013).
7. Z. Sun, D. Popa, T. Hasan, F. Torrisi, F. Wang, E. J. R. Kelleher, J. C. Travers, V. Nicolosi, and A. C. Ferrari, "A stable, wideband tunable, near transform-limited, graphene-mode-locked, ultrafast laser," Nano Res. **3**, 653–660 (2010).
8. F. Bonaccorso, Z. Sun, T. Hasan, and A. Ferrari, "Graphene photonics and optoelectronics," Nat. Photonics **4**, 611–622 (2010).
9. A. K. Geim, "Graphene: status and prospects," Science **324**, 1530–1534 (2009).
10. C. Zhao, H. Zhang, X. Qi, Y. Chen, Z. Wang, S. Wen, and D. Tang, "Ultra-short pulse generation by a topological insulator based saturable absorber," Appl. Phys. Lett. **101**, 211106 (2012).
11. S. Chen, L. Miao, X. Chen, Y. Chen, C. Zhao, S. Datta, Y. Li, Q. Bao, H. Zhang, Y. Liu, S. Wen, and D. Fan, "Few-layer topological insulator for all-optical signal processing using the nonlinear Kerr effect," Adv. Opt. Mater. **3**, 1769–1778 (2015).
12. Y. Chen, G. Jiang, S. Chen, Z. Guo, X. Yu, C. Zhao, H. Zhang, Q. Bao, S. Wen, D. Tang, and D. Fan, "Mechanically exfoliated black phosphorus as a new saturable absorber for both Q-switching and mode-locking laser operation," Opt. Express **23**, 12823–12833 (2015).
13. Z. Bai, G. Tao, Y. Li, J. He, K. Wang, G. Wang, X. Jiang, J. Wang, W. Blau, and L. Zhang, "Fabrication and near-infrared optical responses of 2D periodical Au/ITO nanocomposite arrays," Photon. Res. **5**, 280–286 (2017).
14. Z. Sun, A. Martinez, and F. Wang, "Optical modulators with 2D layered materials," Nat. Photonics **10**, 227–238 (2016).
15. M. Naguib, M. Kurtoglu, V. Presser, J. Lun, J. Niu, M. Heon, L. Hultman, Y. Gogotsi, and M. W. Barsoum, "Two-dimensional nanocrystals produced by exfoliation of Ti_3AlC_2," Adv. Mater. **23**, 4248–4253 (2011).
16. M. Okubo, A. Sugahara, S. Kajiyama, and A. Yamada, "MXene as a charge storage host," Acc. Chem. Res. **51**, 591–599 (2018).
17. X. Wang, S. Kajiyama, H. Iinuma, E. Hosono, S. Oro, I. Moriguchi, M. Okubo, and A. Yamada, "Pseudocapacitance of MXene nanosheets for high-power sodium-ion hybrid capacitors," Nat. Commun. **6**, 6544 (2015).
18. J. Ran, G. Gao, F. T. Li, T. Y. Ma, A. Du, and S. Z. Qiao, "Ti_3C_2 MXene co-catalyst on metal sulfide photo-absorbers for enhanced visible-light photocatalytic hydrogen production," Nat. Commun. **8**, 13907 (2017).
19. H. Lin, X. Wang, L. Yu, Y. Chen, and J. Shi, "Two-dimensional ultrathin MXene ceramic nanosheets for photothermal conversion," Nano Lett. **17**, 384–391 (2017).
20. M. Naguib, V. N. Mochalin, M. W. Barsoum, and Y. Gogotsi, "25th anniversary article: MXenes: a new family of two-dimensional materials," Adv. Mater. **26**, 992–1005 (2014).
21. J. Guo, Y. Sun, B. Liu, Q. Zhang, and Q. Peng, "Two-dimensional scandium-based carbides (MXene): band gap modulation and optical properties," J. Alloys Compd. **712**, 752–759 (2017).
22. B. Anasori, M. R. Lukatskaya, and Y. Gogotsi, "2D metal carbides and nitrides (MXenes) for energy storage," Nat. Rev. Mater. **2**, 16098 (2017).
23. R. Li, L. Zhang, L. Shi, and P. Wang, "MXene Ti_3C_2: an effective 2D light-to-heat conversion material," ACS Nano **11**, 3752–3759 (2017).
24. G. R. Berdiyorov, "Optical properties of functionalized $Ti_3C_2T_2$ (T = F, O, OH) MXene: first-principles calculations," AIP Adv. **6**, 055105 (2016).
25. G. Choi, F. Shahzad, Y.-M. Bahk, Y. M. Jhon, H. Park, M. Alhabeb, B. Anasori, D.-S. Kim, C. M. Koo, Y. Gogotsi, and M. Seo, "Enhanced terahertz shielding of MXenes with nano-metamaterials," Adv. Opt. Mater. **6**, 1701076 (2018).
26. Y. I. Jhon, J. Koo, B. Anasori, M. Seo, J. H. Lee, Y. Gogotsi, and Y. M. Jhon, "Metallic MXene saturable absorber for femtosecond mode-locked lasers," Adv. Mater. **29**, 1702496 (2017).
27. X. Jiang, S. Liu, W. Liang, S. Luo, Z. He, Y. Ge, H. Wang, R. Cao, F. Zhang, Q. Wen, J. Li, Q. Bao, D. Fan, and H. Zhang, "Broadband nonlinear photonics in few-layer MXene $Ti_3C_2T_x$ (T = F, O, or OH)," Laser Photon. Rev. **12**, 1700229 (2018).
28. M. Tuo, C. Xu, H. Mu, X. Bao, Y. Wang, S. Xiao, W. Ma, L. Li, D. Tang, H. Zhang, M. Premaratne, B. Sun, H.-M. Cheng, S. Li, W. Ren, and Q. Bao, "Ultrathin 2D transition metal carbides for ultrafast pulsed fiber lasers," ACS Photon. **5**, 1808–1816 (2018).
29. Y. Dong, S. Chertopalov, K. Maleski, B. Anasori, L. Hu, S. Bhattacharya, A. M. Rao, Y. Gogotsi, V. N. Mochalin, and R. Podila, "Saturable absorption in 2D Ti_3C_2 MXene thin films for passive photonic diodes," Adv. Mater. **30**, 1705714 (2018).
30. X. Wang and Y. Zhou, "Solid-liquid reaction synthesis of layered machinable Ti_3AlC_2 ceramic," J. Mater. Chem. **12**, 455–460 (2002).
31. C. Shi, M. Beidaghi, M. Naguib, O. Mashtalir, Y. Gogotsi, and S. J. Billinge, "Structure of nanocrystalline Ti_3C_2 MXene using atomic pair distribution function," Phys. Rev. Lett. **112**, 125501 (2014).
32. R. Berera, R. van Grondelle, and J. T. Kennis, "Ultrafast transient absorption spectroscopy: principles and application to photosynthetic systems," Photosynth. Res. **101**, 105–118 (2009).
33. M. Holler, F. Schapper, L. Gallmann, and U. Keller, "Attosecond electron wave-packet interference observed by transient absorption," Phys. Rev. Lett. **106**, 123601 (2011).
34. I. H. van Stokkum, D. S. Larsen, and R. van Grondelle, "Global and target analysis of time-resolved spectra," Biochim. Biophys. Acta **1657**, 82–104 (2004).
35. E. Garmire, "Resonant optical nonlinearities in semiconductors," IEEE J. Sel. Top. Quantum Electron. **6**, 1094–1110 (2000).
36. H. Zhang, S. B. Lu, J. Zheng, J. Du, S. C. Wen, D. Y. Tang, and K. P. Loh, "Molybdenum disulfide (MoS_2) as a broadband saturable absorber for ultra-fast photonics," Opt. Express **22**, 7249–7260 (2014).